Active Control of Reheat Buzz

G. J. Bloxsidge,* A. P. Dowling,† N. Hooper,‡ and P. J. Langhorne§
Cambridge University, Cambridge, England, United Kingdom

Reheat buzz is a low-frequency combustion instability involving the propagation of longitudinal pressure waves inside a duct in which a flame is anchored. Active control has been successfully applied to this instability. The controller alters the upstream acoustic boundary condition and thereby changes the energy balance in the duct. Control is found to reduce the peak in the pressure spectrum resulting from combustion instability by 20 dB. The acoustic energy in the whole 0–800-Hz bandwidth is reduced to about 10% of its uncontrolled value. A comparison with numerical calculations is presented.

I. Introduction

REHEAT buzz is the name given to a low-frequency combustion instability of jet aeroengine afterburners. It involves the propagation of longitudinal pressure waves in a duct in which a flame is anchored. Similar pressure waves have been detected on a rig. There, schlieren photographs[1] have shown that these waves perturb the flame, causing it to move and change in surface area, thereby altering the instantaneous rate of heat release. Instability is then possible because, while the acoustic waves perturb the combustion, the unsteady combustion generates yet more sound! If, as discussed by Rayleigh,[2] the unsteady heat release rate is in phase with the pressure perturbations, acoustic waves gain energy from the combustion. Disturbances grow in magnitude if this energy gain is greater than that lost by radiation at the ends of the duct. Strong pressure fluctuations may be set up in this way.

The traditional solution is to reduce the sensitivity of the flame to local flow oscillations (by, for example, redesigning the burner) or to increase the damping in the system. Both these measures have only a limited success and, in some afterburners, the mean rate of heat release must be maintained below a critical level to prevent damage. This condition limits the obtainable thrust augmentation. Active control has recently been demonstrated to be capable of reducing or eliminating thermoacoustic oscillations. It is particularly easy to implement at low frequencies and so complements traditional methods because passive damping is ineffective in this range.

A successful active controller must change the acoustic energy balance within the duct, either by reducing the energy gained by the acoustic waves from the unsteady combustion or by increasing the acoustic energy lost at the boundaries. Both of these methods have been demonstrated to be effective in the control of a Rijke tube.

The Rijke tube is a vertical pipe containing either a heated grid or a flame stabilized by a gauze. It is a simple model burner. Observations show that the Rijke tube may have a thermoacoustic instability when the gauze is in the lower half of the tube but that the flow in the tube is stable whenever the gauze is in the upper half. Rayleigh[2] explained this phenomenon. He noted that the unsteady rate of heat release lags velocity changes. An investigation of the relationship between pressure and velocity perturbations at the pipe's fundamental frequency then shows that the unsteady heat release rate has a component in phase with the pressure oscillations only when the heating element is in the lower half of the tube. It is, therefore, only for these locations that the fundamental mode can grow in amplitude. Such an unstable Rijke tube can be stabilized by the addition of a controlling heater element to the upper part of the pipe. This has been demonstrated by several authors (Collyer and Ayres,[3] Heckl,[4] and Screenivasan et al.[5]). Interestingly, Screenivasan and colleagues note that the power requirement of the controlling heater is considerably less than the power used by the primary heat source (only 3% in some of their experiments). This is because the controller does not need to cancel the effect of the primary source entirely. It needs to reduce the acoustic energy source only to a level below that of the energy losses. Then the perturbations slowly decay.

An alternative form of control is to actively change the boundary conditions of the pipe to increase the loss of acoustic energy. Dines[6] demonstrated this effect by eliminating the instability of a flame burning on a gauze in a Rijke tube. He detected the phase of the disturbances by measuring the light emitted by CH free radicals in the flame. This signal was then passed through a narrow-band filter, phase-shifted, amplified, and fed back to drive a loudspeaker near one end of the tube. A suitable phase delay stabilized the Rijke tube by increasing the energy lost on reflection. Heckl[7] investigated a similar system with a microphone as the detector, instead of the photomultiplier used by Dines. Recently Poinsot et al.[8] have described an experiment to control a turbulent diffusion flame in a tube.

Rayleigh's criterion provides a useful way of investigating the role of a successful active controller for a Rijke tube. However, in an afterburner, there is an appreciable mean rate of heat release and a non-negligible mean flow. In Sec. II, Rayleigh's criterion is extended to describe the energetics of acoustic waves in such a flow.

II. Generalization of Rayleigh's Criterion

Rayleigh[2] gave a clear physical interpretation of the interchange of energy between sound waves and unsteady heating. This was put on a more mathematical basis by Chu.[9] We now extend that work to describe the interaction of one-dimensional acoustic waves with unsteady combustion in a duct with a mean flow and mean heat release.

Consider linear perturbations to a one-dimensional steady flow in a duct of length L with gradually varying cross-sectional area $A(x)$, as shown in Fig. 1. The axial velocity $u(x,t)$ may be decomposed into its mean and fluctuating components,

$$u(x,t) = \bar{u}(x) + u'(x,t)$$

The pressure p, density ρ, and temperature T can be expanded

Presented as AIAA Paper 87-0433 at 25th Aerospace Sciences Meeting, Reno, NV, Jan. 12–15, 1987; received May 11, 1987; revision received Nov. 5, 1987.

*Graduate Student, University Engineering Department.
†Reader, University Engineering Department.
‡Technician, University Engineering Department.
§University Engineering Department; Rolls-Royce Research Fellow, Newnham College.

in a similar way. The heat release rate per unit length of ducting is denoted by

$$Q(x,t) = \bar{Q}(x) + Q'(x,t)$$

The mean values of the equations of mass and momentum conservation yield

$$\frac{\mathrm{d}}{\mathrm{d}x}(\bar{\rho}\bar{u}A) = 0 \tag{1}$$

and

$$\bar{\rho}\bar{u}\frac{\mathrm{d}\bar{u}}{\mathrm{d}x} + \frac{\mathrm{d}\bar{p}}{\mathrm{d}x} = 0 \tag{2}$$

Drag forces have been neglected in the momentum equation. They can be included (see Bloxsidge[10]) but are generally unimportant at the high Reynolds numbers of interest.

For linear one-dimensional perturbations, the mass and momentum equations are

$$A\frac{\partial \rho'}{\partial t} + \frac{\partial}{\partial x}(\rho'\bar{u}A + \bar{\rho}u'A) = 0 \tag{3}$$

and

$$\bar{\rho}\frac{\partial u'}{\partial t} + \bar{\rho}\bar{u}\frac{\partial u'}{\partial x} + (\rho'\bar{u} + \bar{\rho}u')\frac{\mathrm{d}\bar{u}}{\mathrm{d}x} + \frac{\partial p'}{\partial x} = 0 \tag{4}$$

The entropy equation $\rho TA\ \mathrm{D}s/\mathrm{D}t = Q$ may be rewritten as

$$\frac{pA}{R}\frac{\mathrm{D}s}{\mathrm{D}t} = Q \tag{5}$$

where s is the specific entropy, $\mathrm{D}/\mathrm{D}t$ is the material derivative, and the perfect gas equation $\rho T = p/R$ has been assumed. In addition, for a perfect gas, we can write

$$s = c_v \ell n p - c_p \ell n \rho \tag{6}$$

where c_v and c_p are the specific heat capacities at constant volume and pressure, respectively. The mean value of the entropy equation (5) gives

$$\frac{\bar{p}\bar{u}A}{R}\frac{\mathrm{d}\bar{s}}{\mathrm{d}x} = \bar{Q} \tag{7}$$

i.e.,

$$\frac{\bar{p}\bar{u}A}{R}\left(\frac{c_v}{\bar{p}}\frac{\mathrm{d}\bar{p}}{\mathrm{d}x} - \frac{c_p}{\bar{\rho}}\frac{\mathrm{d}\bar{\rho}}{\mathrm{d}x}\right) = \bar{Q} \tag{8}$$

Equations (1), (2), and (8) may be readily solved to determine the development of the mean flow along the duct. They give

$$\frac{\mathrm{d}\bar{u}}{\mathrm{d}x} = -\frac{\bar{u}}{\bar{\rho}}\frac{\mathrm{d}\bar{\rho}}{\mathrm{d}x} - \frac{\bar{u}}{A}\frac{\mathrm{d}A}{\mathrm{d}x}$$

$$= \frac{1}{(1-\bar{M}^2)A}\left[\frac{(\gamma-1)\bar{Q}}{\gamma\bar{p}} - \bar{u}\frac{\mathrm{d}A}{\mathrm{d}x}\right] \tag{9}$$

where $\bar{M} = \bar{u}/\bar{c}$ is the local mean Mach number and γ is the ratio of specific heat capacities.

We now turn our attention to the unsteady flow. With the specific entropy decomposed into mean and fluctuating components, $\bar{s}(x) + s'(x,t)$, the entropy equation (5) states that

$$\frac{\partial s'}{\partial t} + \bar{u}\frac{\partial s'}{\partial x} = \frac{\bar{Q}R}{\bar{p}A}\left(\frac{Q'}{\bar{Q}} - \frac{p'}{\bar{p}} - \frac{u'}{\bar{u}}\right) \tag{10}$$

where, from Eq. (6),

$$\rho' = \frac{p'}{\bar{c}^2} - \frac{\bar{\rho}s'}{c_p} \tag{11}$$

Equation (11) can be used to eliminate the density fluctuation from the unsteady mass and momentum balances, respectively, Eqs. (3) and (4). These become

$$\frac{A}{\bar{c}^2}\frac{\partial p'}{\partial t} + \frac{\partial}{\partial x}(\bar{\rho}u'A) + \frac{\partial}{\partial x}\left(\frac{\bar{u}p'A}{\bar{c}^2}\right) = \frac{\bar{\rho}A}{c_p}\left(\frac{\partial s'}{\partial t} + \bar{u}\frac{\partial s'}{\partial x}\right) \tag{12}$$

and

$$\frac{\partial p'}{\partial x} + \bar{\rho}\frac{\partial u'}{\partial t} + \left(\bar{\rho}u' + \frac{\bar{u}p'}{\bar{c}^2}\right)\frac{\mathrm{d}\bar{u}}{\mathrm{d}x} + \bar{\rho}\bar{u}\frac{\partial u'}{\partial x} = \frac{\bar{\rho}\bar{u}s'}{c_p}\frac{\mathrm{d}\bar{u}}{\mathrm{d}x} \tag{13}$$

It is now possible to construct an acoustic energy equation. Following Morfey,[11] the modified mass and momentum balances are combined by multiplying the mass equation (12) by $(\bar{u}u' + p'/\bar{\rho})$ and adding the result to the product of $(u' + \bar{u}p'/\bar{\rho}\bar{c}^2)A$ and the momentum equation (13). After some algebra, it can be shown that

$$\frac{\partial}{\partial t}(eA) + \frac{\partial}{\partial x}(EA) = (\bar{\rho}\bar{u}\,u' + p')\frac{A}{c_p}\left(\frac{\partial s'}{\partial t} + \bar{u}\frac{\partial s'}{\partial x}\right) + \left(u' + \frac{\bar{u}p'}{\bar{\rho}\bar{c}^2}\right)A\left[\left(\frac{\bar{\rho}s'}{c_p} - \frac{p'}{\bar{c}^2}\right)\bar{u}\frac{\mathrm{d}\bar{u}}{\mathrm{d}x} - \frac{p'}{\bar{\rho}}\frac{\mathrm{d}\bar{\rho}}{\mathrm{d}x}\right] \tag{14}$$

where

$$e = \frac{p'^2}{2\bar{\rho}\bar{c}^2} + \frac{\bar{\rho}u'^2}{2} + \frac{\bar{u}p'u'}{\bar{c}^2}$$

and

$$E = p'u' + \bar{\rho}\bar{u}u'^2 + \frac{\bar{u}^2p'u'}{\bar{c}^2} + \frac{\bar{u}p'^2}{\bar{\rho}\bar{c}^2}$$

To complete the analysis, we substitute for s', $\mathrm{d}\bar{u}/\mathrm{d}x$, and $\mathrm{d}\bar{\rho}/\mathrm{d}x$ from Eqs. (9–11) and integrate along the duct length L to obtain

$$\frac{\partial}{\partial t}\int_0^L eA\,\mathrm{d}x + [EA(L) - EA(0)] = \int_0^L \frac{\gamma-1}{\bar{\rho}\bar{c}^2}Q'(p' + \bar{\rho}\bar{u}u')\,\mathrm{d}x - \int_0^L \frac{(\gamma-1)\bar{Q}}{(1-\bar{M}^2)}\left[(\gamma-1-\gamma\bar{M}^2)\left(\frac{p'^2}{\gamma^2\bar{p}^2} + \frac{\bar{u}p'u'}{\gamma\bar{p}\bar{c}^2}\right) + (1-\bar{M}^2)\frac{u'^2}{\bar{c}^2} + \frac{\bar{M}\rho'}{\bar{\rho}}\left(\frac{u'}{\bar{c}} + \frac{\bar{M}p'}{\gamma\bar{p}}\right)\right]\mathrm{d}x - \int_0^L \frac{\bar{M}^2}{(1-\bar{M}^2)}(\bar{u}p' + \bar{\rho}\bar{c}^2u')\frac{s'}{c_p}\frac{\mathrm{d}A}{\mathrm{d}x}\,\mathrm{d}x \tag{15}$$

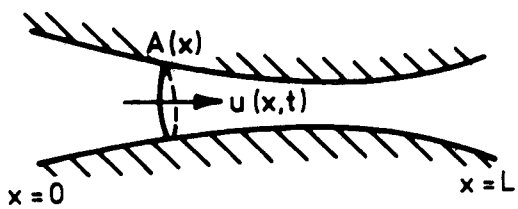

Fig. 1 A duct of slowly varying cross-sectional area with mean flow and mean heat release.

We see that $e(x)$ and $E(x)$ are the generalized acoustic energy density and energy flux respectively. As pointed out by Morfey,[11] the forms for e and E have some intuitive appeal. In the absence of a mean flow, they reduce to the standard acoustic energy density and intensity. Moreover, e is positive definite for a subsonic flow whereas E allows no acoustic energy flow upstream across a choked nozzle. Also, they agree with Blokhintsev's expressions[12] in the geometrical acoustics limit.

The first source term on the right-hand side of Eq. (15) describes the acoustic energy generated by unsteady combustion. The second integral accounts for the energy produced by interaction between the mean heat release rate and acoustic perturbations. The last term describes the well-known effect that sound is generated as entropy fluctuations are convected through an area change (see, for example, Ffowcs Williams and Howe[13]).

The source terms on the right-hand side of Eq. (15) appear to be somewhat unwieldy. However, in our experimental investigation of reheat buzz, we have found $Q'/\bar{Q}$ to be of order $u'/\bar{u}$, which is much larger than either $p'/\bar{p}$ or $u'/\bar{c}$ in a low Mach number flow. When terms of order $\bar{M}$ are neglected in comparison with unity, the right-hand side of Eq. (15) simplifies and, for a straight-walled duct, we obtain the usual Rayleigh source term,

$$\frac{\partial}{\partial t}\int_0^L eA\,\mathrm{d}x + [EA(L) - EA(0)] = \int_0^L \frac{(\gamma-1)}{\bar{\rho}\bar{c}^2}\,Q'p'\,\mathrm{d}x \quad (16)$$

Equation (16) states that disturbances grow if their net energy gain from the combustion is greater than the sum of their energy losses across the boundary. Therefore, the acoustic mode grows in amplitude if

$$\int_0^L \frac{(\gamma-1)}{\bar{\rho}\bar{c}^2}\,\overline{Q'p'}\,\mathrm{d}x > [\bar{E}A(L) - \bar{E}A(0)] \quad (17)$$

where the overbar denotes an average over one period of the acoustic oscillation. This is a generalized form of Rayleigh's criterion. When it is satisfied, the combustor has a thermoacoustic instability, and linear waves increase in amplitude until limited by nonlinear effects.

III. Active Control of Reheat Buzz

A rig has been set up at Cambridge to model an afterburner and investigate reheat buzz. The geometry is illustrated in Fig. 2. A flame is stabilized behind a conical gutter, and the whole burning length is visible through quartz ducting. Air is supplied at constant pressure to a choked nozzle at the upstream end of the working section. In a similar way, the fuel (ethylene) is injected at constant temperature and pressure through choked holes. The fuel and air mix effectively in the nozzle, thus supplying a premixed gas of uniform fuel-air ratio and constant mass flow rate to the working section. At a typical running condition, the mean flow velocity upstream of the flame is 27 m/s, and about 0.25 MW of heat is released in the duct. The oscillations in the flow are monitored by recording the unsteady pressures $p'(x,t)$ at various axial positions along the duct. In addition, following Hurle et al.,[14] the light emission from C_2 radicals in the flame is measured. The optical arrangement is straightforward. A screen blanks off all but a 100-mm length of flame. An image of this portion is focused through a filter onto the photocathode of a photomultiplier. The filter is centered on 516.7 nm with a bandwidth of 3.2 nm to pass the light emitted in the main C_2 transition. Previous work on this rig[10] has shown that the heat release may be assumed to be proportional to this light emission. We denote the output from the photomultiplier, as it receives filtered light from a 100-mm window, by $I(x,t)$, where x is the axial position of the center of the window.

The upstream end of the working section is choked, and its downstream end is open. These boundary conditions mean that the fundamental mode shape is approximately a quarter-wave, and measurements show p' and Q' to be in phase along most of the burning length. It is then evident from the inequality in Eq. (17) that the driving toward instability is strong and, indeed, the observed sound pressure levels can exceed 160 dB. Because the mode is a quarter-wave, p' and Q' are in phase for any position of the gutter, and the instability cannot be eliminated by introducing a second burner as for the Rijke tube. Attempts at control have, therefore, concentrated on actively changing the boundary condition.

For active control, the fixed choked nozzle is replaced by a choked plate and a movable centerbody, which can be oscillated axially to modify the upstream acoustic boundary condition, as illustrated in Fig. 3. The choked plate ensures that the mean flow supplied to the rig is unchanged when the controller is switched on. A pressure signal that has been filtered and phase-shifted using analog components is fed into a 300-W commercial vibrator. This in turn oscillates the centerbody via a mechanical linkage. Axial motion of the shaped centerbody alters the blockage to the flow, thereby producing a fluctuating mass flow into the working section and modifying the upstream acoustic boundary condition.

The active control experiments were performed for the geometry shown in Fig. 3 at an inlet Mach number of 0.08, inlet stagnation temperature of 288 K, and an equivalence ratio of 0.663 (i.e., the fuel-air ratio is 66.3% of the stoichiometric fuel-air ratio). The flow perturbations in the controlled case are compared with those that occur when the centerbody is clamped at the same mean position with the same fuel flow and airflow rates. In this rigid uncontrolled case, the pressure spectrum measured by a transducer upstream of the flame is found to have a strong peak at 88 Hz (see Fig. 4). This is the frequency of the combustion instability.

The feedback circuitry is required to filter and phase-shift the signal from the pressure transducer. Although this feedback circuit is the same in principle at that used by Dines[6] and Heckl,[7] several modifications were needed in practice. In particular, the buzz instability, unlike the simple Rijke tube oscillation, has significant cycle-to-cycle variations. The narrow-band feedback circuit used by Dines and Heckl involves too much delay to control these nonstationary oscillations. In order to minimize the time delay, a broadband controller was used but this, in turn, brought its own problems. The first design of feedback circuit enabled the optimum phase shift across the feedback circuit to be determined. But, as the gain was increased, a feedback instability was introduced, thereby limiting the overall improvement possible. The information gleaned from this prototype controller led to the design of a new controller with improved performance.[15] The revised controller consists of a differentiator and a high-pass Butterworth filter set with

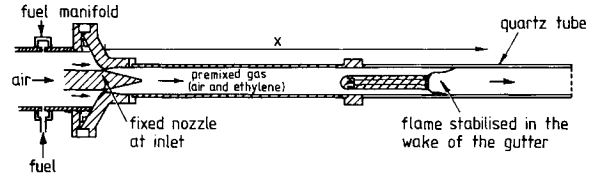

Fig. 2 Geometry of the Cambridge reheat buzz rig.

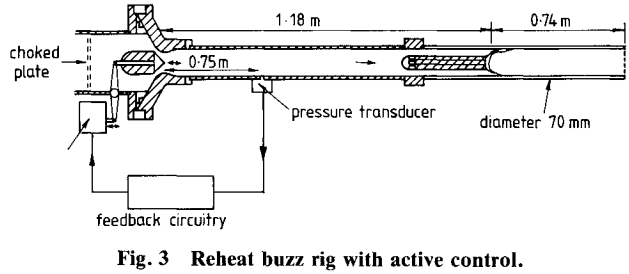

Fig. 3 Reheat buzz rig with active control.

a cutoff frequency of 40 Hz. Together, these two components produce the required phase change at the frequency of the combustion instability. They also have the advantage of attenuating the low-frequency input to the vibrator. The centerbody and the flow respond with large amplitudes at low frequencies, and there is again the possibility of a feedback instability without some high-pass filtering.

Figure 4 shows results obtained with the improved controller. As one might expect, the change in the upstream boundary condition has altered the frequency of the peak in the pressure spectrum. It has also significantly reduced its amplitude. The second harmonic has been completely eliminated. Indeed, the acoustic power in the 0–800-Hz bandwidth has been reduced to 11% of the power at the same mean flow conditions but with a fixed upstream nozzle. The pressure spectrum is shown with greater resolution in Fig. 5 for the 50–150-Hz frequency range. With the improved controller, there is no predominant peak left in the pressure spectrum. Analysis of the spectrum at a number of positions along the duct indicates small peaks at 69, 79, and 108 Hz. Of these, only the 79-Hz peak exists in all the pressure spectra and has a corresponding peak in the light emission, indicating that this is the controlled combustion instability.

Figure 6 shows the time history of oscillations in the duct. Cycle-to-cycle variations, even in the controlled case, can be seen clearly. When the control signal is switched off, perturbations grow rapidly until a nonlinear limit cycle with increased amplitude is attained.

The active control has succeeded in considerably reducing the low-frequency perturbations in the duct. This means that an engine could be run at a higher fuel-air ratio without damage. A further advantage is illustrated in Fig. 7. The mean light emitted by 100-mm lengths of flame, with and without control, is plotted as a function of the position of the window center. It is clear that considerably more light is emitted in the controlled case than without control. In fact, the light output from the first five windows is increased by about 23% by the active control. A corresponding increase in heat output can be expected. Indeed, it was impossible to obtain light readings from the combustion within the last 200 mm of the duct with control because the end of the duct was so hot it was glowing! Nevertheless, we may conclude that without control the combustion within the duct is incomplete. The active control significantly increases the combustion within the duct, which leads to a corresponding increase in thrust. Alternatively, the same thrust could be obtained from a shorter duct length by using active control. Both these conclusions have important implications for afterburners.

The time history of the light emission in Fig. 6 shows more clearly how the control affects the mean light and hence the mean heat release rate. The peak light output in one period of oscillation is seen to be the same with and without control. The larger oscillations in the uncontrolled case lead to a greater reduction from the peak value during the cycle, with a corresponding decrease in the mean light emission.

The light emission system can be calibrated. If we assume that the heat release rate is proportional to the light output, a measurement of exit temperature leads to a calibration of about 6.5 kW/V.

At the frequency of the combustion instability, there is good coherence between the pressure and the light emission along the

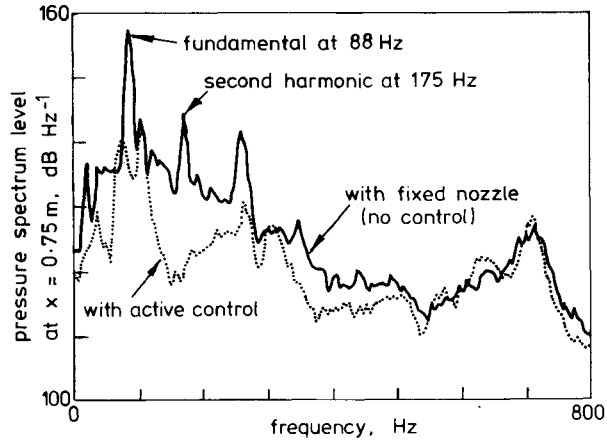

Fig. 4 Effect of active control on the pressure spectrum (0–800-Hz bandwidth).

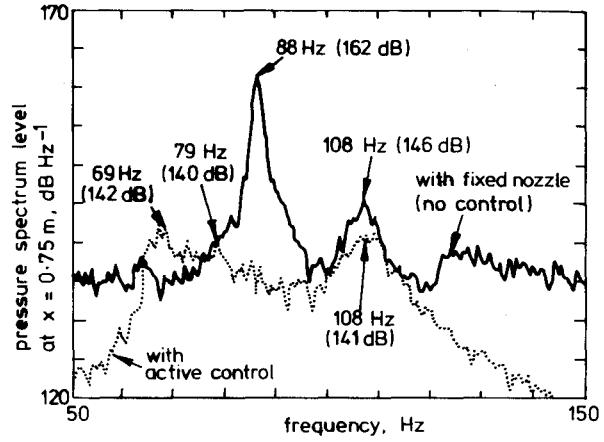

Fig. 5 Effect of active control on the pressure spectrum (improved resolution).

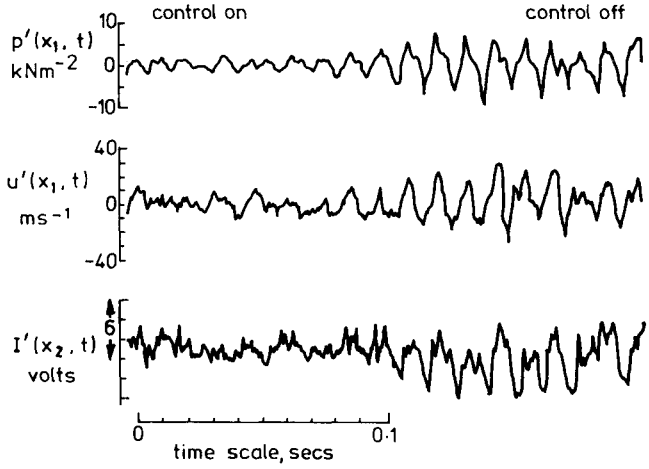

Fig. 6 Time history of oscillations in the duct, $x_1 = 0.75$ m, $x_2 = 1.52$ m.

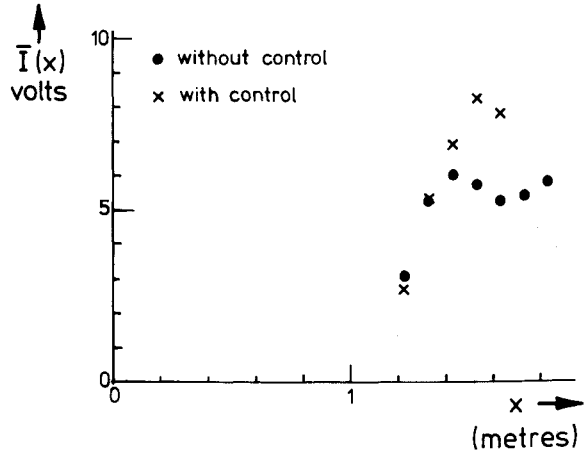

Fig. 7 Mean light emitted by 100-mm lengths of flame with and without control as a function of x, the axial position of the center of the window.

duct. A set of transfer functions can therefore be measured. The pressure signal at $x = x_{ref}$, 0.75 m downstream of the nozzle, is taken as the reference signal. Figures 8 and 9 show measurements of the relative magnitude and phase of the pressures at x and x_{ref} without and with control, respectively. The relative magnitude and phase of the light emitted in 100-mm windows are also plotted as a function of the position of the center of the window. It is apparent that the pressure and heat release are nearly in phase at the frequency of the combustion instability. There is therefore driving toward instability.

The Rayleigh source term,

$$(\gamma - 1) \int_0^L (\overline{p'Q'}/\bar{\rho}\bar{c}^2)\, dx$$

can be estimated. The data in Figs. 5, 8, and 9 and the calibration of the photomultiplier output give the unsteady heat output in each 100-mm window. When this is multiplied by an average pressure perturbation for each window and the cosine of the phase difference, it leads to the power spectral density of the Rayleigh driving term at the frequency of the combustion instability. It is found that

$$(\gamma - 1) \int_0^L \frac{\overline{p'Q'}}{\bar{\rho}\bar{c}^2}\, dx \sim 190 \text{ W/Hz without control} \quad (18a)$$

$$\sim 2.5 \text{ W/Hz with control} \quad (18b)$$

The control significantly reduces the energy that the acoustic waves gain from the combustion, mainly because the amplitude of the fluctuations has been effectively reduced.

Figures 10 and 11 show the effects of changes in the feedback circuit. The gain across the circuit was reduced to obtain Fig. 10, which demonstrates that, at low levels of gain, the controller becomes more effective as the gain is increased. At higher levels, however, a further increase in gain has little effect.

The phase change across the feedback circuit may be altered by introducing an additional element that produces an adjustable time delay. Figure 11 shows the effects of such changes in phase. The optimum is the design case. But the controller is found to attenuate the combustion instability to some extent for a range of phases (almost 170 deg). This is an encouraging result because it means that the controller need not be set very accurately to be effective. This is in contrast to conventional antisound, where a new sound wave must be introduced almost exactly out of phase with an existing wave if there is to be significant reduction. In our case, the feedback circuit is simply required to increase the acoustic energy radiated from the duct ends. This may be achieved with a range of phase changes across the feedback circuit. It is apparent from Fig. 12 that there are phase changes that can increase the amplitude of the combustion instability, but experimental difficulties meant that this region was not fully explored! The difference shown in the performance of the controller between phase changes near ± 180 deg emphasizes the importance of reducing the overall time delay in the circuit. The control signal with phases plotted near − 180 deg is delayed by almost a cycle in comparison with those near + 180 deg. There is a significant degradation in performance.

An analysis has been developed to determine the frequency and mode shape of the low-frequency combustion instability in a duct with a fixed choked upstream end. This theory can be extended to describe the oscillations with the feedback circuit.

IV. Comparison with Theory

The theory is a linear stability analysis of the flow within the duct.[10] Because the theory is linear, each Fourier component may be considered separately, and it is sufficient to investigate perturbations to the mean flow with time dependence $e^{i\omega t}$. We find the eigenfrequencies ω for which the acoustic boundary conditions at both ends of the duct are satisfied. The real part of ω then specifies the frequency of this mode, while the sign of the imaginary part of ω determines whether linear disturbances grow or decay. The frequencies of interest are low, with wavelengths long in comparison with the duct diameter. This means that only plane acoustic waves carry energy, and we, therefore, consider the flow to be one-dimensional. The axial velocity $u(x,t)$ may be decomposed into its mean and fluctuating components:

$$u(x,t) = \bar{u}(x) + u'(x,t)$$

with

$$u'(x,t) = Re[\hat{u}(x)e^{i\omega t}]$$

The pressure, density, temperature, and heat release rate per unit length of ducting Q can be expanded in a similar way.

The relationship between $Q(x,t)$ and the flow has been investigated in previous experiments on this rig.[10] There it was noted that the variation of $\bar{Q}$ with axial position x may be approximated by two straight lines:

$$\bar{Q}(x) = B(x - x_G)/(x_R - x_G) \quad \text{for } x < x_R \quad (19a)$$

$$= B + C(x - x_R)/(L - x_R) \quad \text{for } x > x_R \quad (19b)$$

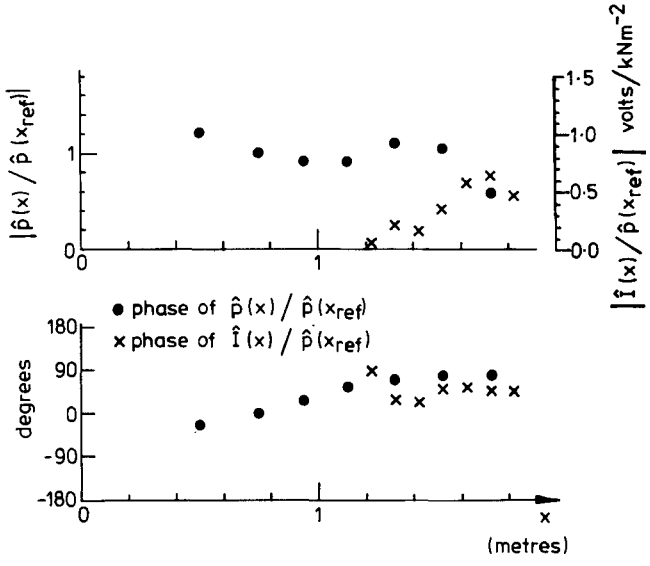

Fig. 8 Variation of pressure and light emission along the duct at the buzz frequency without control.

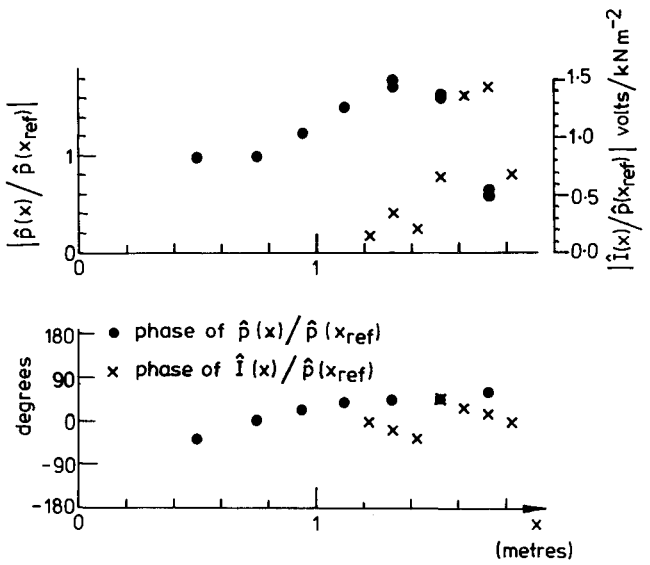

Fig. 9 Variation of pressure and light emission along the duct at the 'buzz' frequency with control.

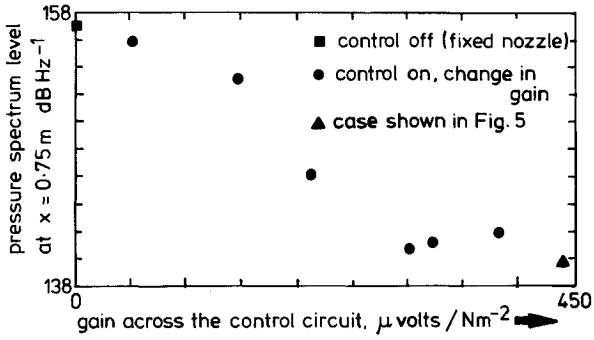

Fig. 10 Effect of altering the gain across the feedback circuit.

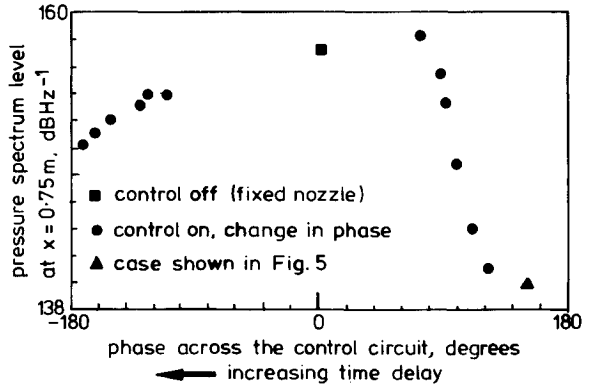

Fig. 11 Effect of altering the phase across the feedback circuit.

Here, x_G denotes the position of the downstream end of the gutter, and x_R is four duct diameters downstream of x_G and is near the end of the recirculation zone.[16] The open end of the duct is at L. B and C are functions of fuel-air ratio.

The unsteadiness in the heat release rate is more important to an understanding of combustion instabilities because, as shown by Rayleigh's criterion, this is the term that provides the driving mechanism for the perturbations. The relationship between $Q'(x,t)$ and the unsteady flow has been thoroughly investigated by exciting a stable flame with sound waves.[8] The rig was run at a low fuel-air ratio for which the flame was stable. Then, sound waves of various frequencies ω were generated and the unsteady heat released in response to these flow perturbations measured. It was found that changes in heat release rate propagate down the duct and that, apart from this time delay, they related to velocity perturbations at the gutter lip, $\hat{u}_G$, i.e.,

$$\frac{\hat{Q}(x)}{\bar{Q}(x)} = f\left(\frac{\omega d}{\bar{u}_G}\right)\frac{\hat{u}_G}{\bar{u}_G}\,e^{-i\omega\tau(x)} \tag{20}$$

where $\tau(x)$ is the time taken for disturbances to travel downstream from the gutter to x, and d is the diameter of the gutter; f is a function of the Strouhal number $\omega d/\bar{u}_G$ and, in the range of frequencies of interest, this function is approximately $\bar{u}_G/i\pi\omega d$. Equation (20) then reduces to a statement that

$$\frac{\hat{Q}(x)}{\bar{Q}(x)} = \frac{\hat{u}_G}{i\pi\omega d}\,e^{-i\omega\tau(x)} = \frac{\hat{\eta}_G}{\pi d}\,e^{-i\omega\tau(x)} \tag{21}$$

Apart from a time delay, the unsteady heat release rate depends on η_G, the perturbation in particle displacement at the gutter, divided by the circumference of the gutter lip.

The empirical model of flame response expressed in Eqs. (19–21) was developed to describe combustion instabilities in the basic configuration shown in Fig. 2, where there is a choked nozzle upstream of the working section. The model has been used with some success for such a geometry with a range of duct lengths and flow conditions.[10] We will now test the same flame model still further by applying it to the active control geometry.

When $Q(x,t)$ is specified as a function of the flow, the mean and unsteady flow in the duct may be calculated. In sections of the duct with uniform cross-sectional area A, the mean values of the equations of mass, momentum, and energy are

$$\frac{\mathrm{d}}{\mathrm{d}x}(\bar{\rho}\bar{u}) = 0 \tag{22a}$$

$$\frac{\mathrm{d}}{\mathrm{d}x}(\bar{p} + \bar{\rho}\bar{u}^2) = 0 \tag{22b}$$

$$\frac{\mathrm{d}}{\mathrm{d}x}[\bar{\rho}\bar{u}A(c_p\bar{T} + \tfrac{1}{2}\bar{u}^2)] = \bar{Q} \tag{22c}$$

At the upstream end of the stem supporting the gutter and at the gutter itself, the duct area available to the flow abruptly decreases, and a force is exerted on the fluid. The change in the mean flow across these contractions can be calculated from the equations of conservation of mass and energy flux and the fact that the flow is isentropic.

It is not reasonable to assume that the flow is one-dimensional just downstream of the gutter. Instead, this region is enclosed by a control volume, and equations of conservation of mass, momentum, and energy are applied across it. These, together with a Kutta condition that pressure is uniform across the upstream surface of the control volume, enable the downstream flow to be calculated in terms of the upstream flow.

If the mean flow is known at one axial position, Eq. (22) may be integrated with respect to x and, together with the jump conditions across the control volumes, determine the flow farther downstream. The mean flow actually satisfies mixed point boundary conditions. The inlet Mach number and temperature are known, and the exit pressure is atmospheric. The scheme adopted is to guess the upstream mean pressure, integrate down the duct, and then iterate in the value of the upstream guess for pressure until the exit pressure is atmospheric. Then, the mean flow throughout the duct is determined.

The unsteady flow may be calculated in a similar way. The equations of mass, momentum, and energy conservation for linear perturbations of frequency ω, in a duct of uniform area A, are

$$\frac{\mathrm{d}}{\mathrm{d}x}(\hat{\rho}\bar{u} + \bar{\rho}\hat{u}) = -i\omega\hat{\rho} \tag{23a}$$

$$\frac{\mathrm{d}}{\mathrm{d}x}(\hat{p} + \hat{\rho}\bar{u}^2 + 2\bar{\rho}\bar{u}\hat{u}) = -i\omega(\hat{\rho}\bar{u} + \bar{\rho}\hat{u}) \tag{23b}$$

and

$$A\frac{\mathrm{d}}{\mathrm{d}x}\{(\hat{\rho}\bar{u} + \bar{\rho}\hat{u})(c_p\bar{T} + \tfrac{1}{2}\bar{u}^2) + \bar{\rho}\bar{u}(c_p\hat{T} + \bar{u}\hat{u})\}$$

$$= \hat{Q} - i\omega A\{\hat{\rho}(c_v\bar{T} + \tfrac{1}{2}\bar{u}^2) + \bar{\rho}(c_v\hat{T} + \bar{u}\hat{u})\} \tag{23c}$$

These may be readily integrated along straight portions of the duct to describe the development of the perturbations. Again, across abrupt contractions in duct area, we use conservation of mass and energy and the fact that the flow is isentropic. Similarly, conservation of mass, momentum, and energy are applied across the control volume downstream of the gutter lip.

The upstream acoustic boundary conditions are somewhat complicated. There is a perforated plate with choked holes and a nozzle with either a clamped or oscillating centerbody. Rather than attempt to calculate the reflection of acoustic waves from such an arrangement, we have taken a pragmatic view and measured it. The impedance $\hat{p}/\hat{u}$ was measured at the reference position x_{ref} upstream of the flame. It was found that

$$\hat{p}(x_{ref}) = 331e^{i158\,deg}\ Nm^{-2}/ms^{-1} \text{ for no control, fixed nozzle} \quad (24a)$$

$$\hat{u}(x_{ref}) = 242e^{-i159\,deg}\ Nm^{-2}/ms^{-1} \text{ for the optimum control case shown in Fig. 5} \quad (24b)$$

In addition, we assume the flow to be isentropic upstream of the flame. The flow perturbations are therefore known at x_{ref} and, for a prescribed value of ω, Eq. (23) may be integrated in both directions to obtain the development of the unsteady flow. There is an open end downstream of the working section, and we apply Howe's[17] boundary condition there. This boundary condition includes end corrections owing to finite mean velocity and duct diameter but actually, for the values of these parameters in our rig, it differs little from $p'(L) = 0$. The boundary condition will not be satisfied for a general ω. Iteration in the value of ω to meet this condition determines the eigenfrequency. The mode shape is also calculated.

Figures 12 and 13 show results obtained by this calculation procedure. With the control switched off and the centerbody clamped, the eigenfrequency is found to have a negative imaginary part. This means that, according to linear theory, disturbances grow exponentially with time and the flow is unstable. In practice, perturbations increase in amplitude until limited by nonlinear effects. Figure 12 compares the calculated mode shape for the pressure fluctuations with the measured values displayed in Fig. 8. There is excellent agreement, although the calculated frequency 95.6 Hz differs by 8% from the measured value of 88 Hz.

With the control switched on, the changed upstream boundary condition alters both mode shape and frequency. Now ω is found to have a positive imaginary part, indicating that the flow has been stabilized. Figure 13 compares the calculated mode shape with the experimental data of Fig. 9. Once again, the agreement is good. The calculated frequency of 78.0 Hz is in excellent agreement with the measured value of 79 Hz.

The comparison between theoretical and measured pressure perturbations is so good that we can have some confidence that the flow is being calculated accurately. The calculated values for the flow at the ends of the duct will therefore be used to investigate the radiation loss. Since the theory is linear, it leads only to mode shapes and not absolute values. How- ever, the flow at the ends of the duct is completely determined by the calculated transfer functions $\hat{p}(x)/\hat{p}(x_{ref})$, $\hat{u}(x)/\hat{p}(x_{ref})$, $\hat{\rho}(x)/\hat{p}(x_{ref})$ and the measured power spectral density at x_{ref}. Equation (16) showed the power flow from the ends of the duct to be $AE(L)$ and $AE(0)$, where

$$E = p'u' + \bar{\rho}\bar{u}u'^2 + \frac{\bar{u}^2p'u'}{\bar{c}^2} + \frac{\bar{u}p'^2}{\bar{\rho}\bar{c}^2}$$

The spectral density of this power flow at the frequency of the combustion oscillation has been calculated.[10] For the fixed centerbody, the spectral density of the sound power propagating upstream is found to be 55 W/Hz compared with only 0.4 W/Hz when the active control is on, while the energy flow through the hot, open end is 140 W/Hz for the fixed centerbody and 2.0 W/Hz with control. So, proportionally more (almost twice as much) acoustic energy is lost at the downstream end as the control is switched on. The active control works by increasing the relative magnitude of the flux of generalized acoustic energy at the hot end of the duct. This is achieved by altering the upstream boundary condition on which the fundamental frequency and mode shapes depend, thus altering the energy flux at the downstream exit, which is itself a function of frequency.

There is a reassuring balance of energy in the limit cycles. The magnitude of the calculated energy lost by radiation without and with control is 195 W/Hz and 2.4 W/Hz, respectively. Equation (16) indicates that this should be equal to the energy gained from the Rayleigh source, and indeed it is. The power spectral density of the acoustic energy gained from the combustion without and with control was estimated from

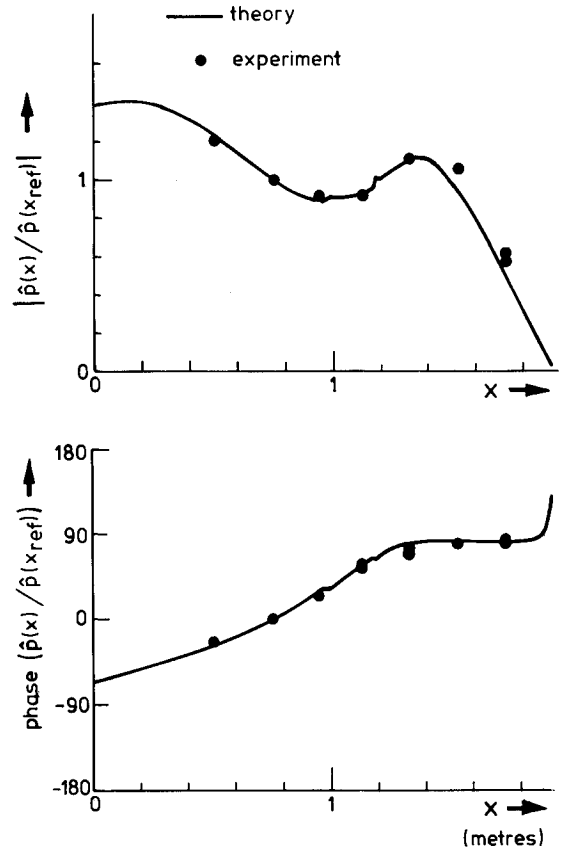

Fig. 12 Variation in the pressure along the duct at the buzz frequency without control; comparison of theory and experiment.

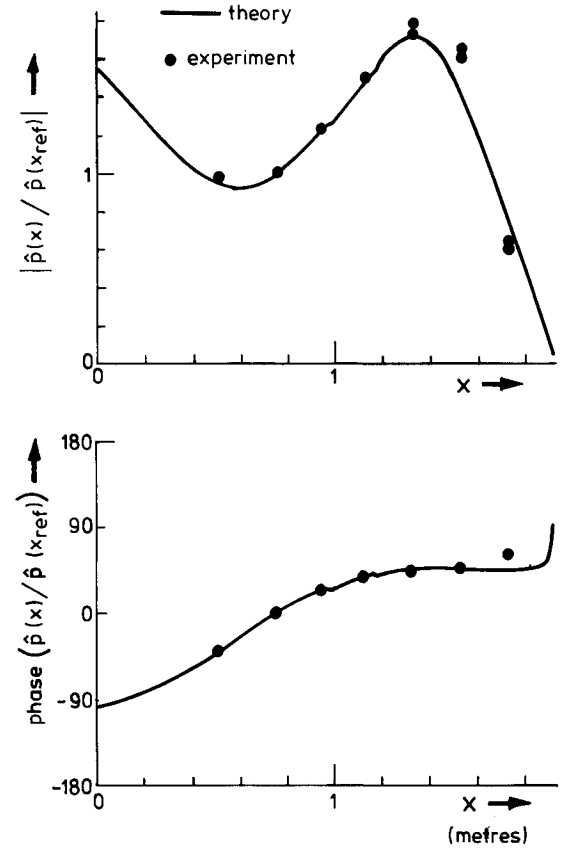

Fig. 13 Variation in the pressure along the duct at the buzz frequency for the optimum control case; comparison of theory and experiment.

measurements in Eq. (18) to be 190 W/Hz and 2.5 W/Hz. This is equal to the corresponding radiation loss, at least to the order of accuracy of the estimates.

V. Conclusions

Combustion oscillations in a 0.25-MW burner have been stabilized by active control. Comparison with theory shows that such stability can be satisfactorily explained by assuming the active control to alter the boundary conditions and so change the energy balance of acoustic waves within the burner.

Work is currently in progress on more practical ways of implementing the feedback, but there is already sufficient evidence to conclude that active control can provide a useful technique, complimentary to conventional methods, in the reduction of damaging thermoacoustic fluctuations.

Acknowledgments

Helpful discussions with Professor J. E. Ffowcs Williams and Dr. K. Glover are gratefully acknowledged. This work was funded by Rolls-Royce PLC and carried out, while one of the authors (GJB) was in receipt of a Science and Engineering Research Council studentship.

References

[1]Smart, A. E., Jones, B., and Jewell, N. T., "Measurements of Unsteady Parameters in a Rig Designed to Study Reheat Combustion Instabilities," AIAA Paper 76-141, 1976.

[2]Rayleigh, J. W. S., *The Theory of Sound: Vol. II,* Dover, New York, 1945.

[3]Collyer, A. A. and Ayres, D. J., "The Generation of Sound in a Rijke Tube Using Two Heating Coils," *Journal of Physics,* Series D, Vol. 5, 1972, pp. L73–L75.

[4]Heckl, M. A., "Heat Sources in Acoustic Resonators," Ph.D. Thesis, Cambridge University, Cambridge, England, 1985.

[5]Screenivasan, K. R., Raghu, S., and Chu, B. T., "The Control of Pressure Oscillations in Combustion and Fluid Dynamical Systems," AIAA Paper 85-0540, 1985.

[6]Dines, P. J., "Active Control of Flame Noise," Ph.D. Thesis, Cambridge University, Cambridge, England, 1983.

[7]Heckl, M. A., "Active Control of the Noise from a Rijke Tube," *IUTAM Symposium on Aero and Hydro-acoustics*, Springer-Verlag, New York, 1986.

[8]Poinsot, T., Bourienne, F., Esposito, E., Candel, S., and Lang, W., "Suppression of Combustion Instabilities by Active Control," AIAA Paper 87-1876, July 1987.

[9]Chu, B. T., "On the Energy Transfer to Small Disturbances in Fluid Flow (Part I)," *Acta Mechanica*, Vol. 1, 1964, pp. 215–234.

[10]Bloxsidge, G. J., "Reheat Buzz—An Acoustically Driven Combustion Instability," Ph.D. Thesis, Cambridge University, Cambridge, England, 1987.

[11]Morfey, C. L., "Acoustic Energy in Non-Uniform Flows," *Journal of Sound and Vibration*, Vol. 14, Pt. 2, 1971, pp. 159–170.

[12]Blokhintsev, D. I., "Acoustics of a Non-Homogeneous Moving Medium," NACA TM-1399, 1946.

[13]Ffowcs Williams, J. E. and Howe, M. S., "The Generation of Sound by Density Inhomogeneities in Low Mach Number Flow," *Journal of Fluid Mechanics*, Vol. 70, Pt. 3, 1975, pp. 605–622.

[14]Hurle, I. R., Price, R. B., Sugden, T. M., and Thomas, A., "Sound Emission from Open Turbulent Premixed Flames," *Proceedings of the Royal Society of London,* Series A, Vol. 303, 1986, pp. 409–427.

[15]Bloxsidge, G. J., Dowling, A. P., Hooper, N., and Langhorne, P. J., "Active Control of an Acoustically Driven Combustion Instability," *Journal of Theoretical and Applied Mechanics* (special issue, supplement to Vol. 6), 1987, pp. 161–175.

[16]Zukoski, E., "Afterburners" in *The Aerothermodynamics of Aircraft Gas Turbine Engines*, edited by G. C. Oates, Air Force Aero Propulsion Lab., TR-78-52, 1978, Chap. 21.

[17]Howe, M. S., "Attenuation of Sound in a Low Mach Number Nozzle Flow," *Journal of Fluid Mechanics*, Vol. 91, Pt. 2, 1979, pp. 209–229.